AD-A269 739

ELECTRICAL PROPERTIES OF REDISPERSED IRON FIBERS MEASURED AT 94 GHz

C. W. Bruce
U.S. Army Research Laboratory

A. V. Jelinek and P. A. Silva
Physical Science Laboratory

ARL-TR-59

August 1993

[illegible] findings in this report are not to be construed as an official Department of the Army position, unless so designated by other authorized documents.

The use of trade names and names of manufacturers in this report is not to be construed as official Government indorsement or approval of commercial products or services referenced herein.

Destruction Notice

When this document is no longer needed, destroy it by any method that will prevent disclosure of its contents or reconstruction of the document.

REPORT DOCUMENTATION PAGE

Form Approved
OMB No 0704-0188

1. AGENCY USE ONLY (Leave blank)	2. REPORT DATE	3. REPORT TYPE AND DATES COVERED
	August 1993	Final

4. TITLE AND SUBTITLE

OPTICAL PROPERTIES OF RED..'ERSED IRON FIBERS MEASURED AT 94 GHZ

5. FUNDING NUMBERS

6. AUTHOR(S)

C. W. Bruce,
*A. V. Jelinek and P. A. Silva

7. PERFORMING ORGANIZATION NAME(S) AND ADDRESS(ES)

U.S. Army Research Laboratory
Battlefield Environment Directorate
ATTN: AMSRL-BE-A
White Sands Missile Range. NM 88002-5501

8. PERFORMING ORGANIZATION REPORT NUMBER

ARL-TR-59

9. SPONSORING/MONITORING AGENCY NAME(S) AND ADDRESS(ES)

U.S. Army Research Laboratory
2800 Powder Mill Road
Adelphi, MD 20783-1145

10. SPONSORING/MONITORING AGENCY REPORT NUMBER

11. SUPPLEMENTARY NOTES

*Physical Science Laboratory
New Mexico State University
Las Cruces, New Mexico 88003

12a. DISTRIBUTION/AVAILABILITY STATEMENT

Approved for public release; distribution is unlimited.

12b. DISTRIBUTION CODE

13. ABSTRACT (Maximum 200 words)

Millimeter wavelength attenuative properties of iron fibers produced by the high temperature reduction of iron carbonyl were measured in both controlled and field environments. Aerosol morphology was evaluated statistically for the controlled studies, and results were used as a basis for calculations of the absorption efficiency. Scattering efficiency for such small diameter fibers can be assumed to be a negligible proportion of the net attenuation. Reasonable agreement between measurements and theory is indicated. Efficiencies remain relatively high for visible wavelengths.

14. SUBJECT TERMS

Extinction, absorption, iron, fibers

15. NUMBER OF PAGES
17

16. PRICE CODE

17. SECURITY CLASSIFICATION OF REPORT	18. SECURITY CLASSIFICATION OF THIS PAGE	19. SECURITY CLASSIFICATION OF ABSTRACT	20. LIMITATION OF ABSTRACT
Unclassified	Unclassified	Unclassified	SAR

Contents

List of Figures

1. Introduction

This report gives results of laboratory and field measurements of the millimeter wavelength optical properties of iron fibers at 94 GHz. These fibers are produced by the high temperature reduction of $Fe(CO)_5$ to iron condensate spherules (diameter $\approx 0.1\ \mu m$) which coalesce in the final stages of their growth to form chains or fibers. In the presence of a magnetic field, they become quite straight; otherwise they would closely resemble, for a common example, carbonaceous soot. Examples of the iron fibers are shown in figure 1.*

The laboratory measurements were performed under carefully controlled conditions using redispersed fibers. Since the laboratory aerosol was well characterized, one can estimate the optical result using either the ellipsoidal theory or a much more precise theory by Pedersen et al. (1985, 1987) and Waterman and Pedersen (1992). The agreement for the latter was well within the limits of the uncertainty and suggested the potential for very high extinction (absorption) efficiency for longer fibers. However, it has not been established that the longer iron fibers have the strength to withstand redispersal.

Field measurements of iron fibers generated in-situ are also included and remind the reader of another feature predicted by the theory (Waterman and Pedersen 1992, van de Hulst 1957) for this aerosol; that is, the extinction efficiencies at the short wavelengths (visible, infrared (IR)) are even higher than those for the millimeter wavelengths. This, of course, is reversed for the 3- to 10-μm diameter graphitic particles (Bruce et al. 1990a, 1990b). Unfortunately, because of inadequate characterization (sample oxidized on the substrates) and particle geometrical complexity (multiple connectedness, nesting) for these iron fiber experiments (1984), meaningful comparison with the theory is not feasible.

2. Definitions

Since the research of this group involves both of the components of the extinction, the usual definition of small alpha for the latter quantity is inconvenient. Therefore, the symbols will be defined as follows. T, the transmissivity over the pathlength l is defined by

$$T = e^{-\int \epsilon dl}$$

*Figures are located at the end of the report.

where

$$\varepsilon = \rho\epsilon$$

Small epsilon, $\epsilon(m^2/g)$, is the extinction efficiency defined as the extinction coefficient, $\varepsilon(m^{-1})$, divided by the mass density, $\rho(g/m^3)$, of the aerosol in a volume of space. Then,

$$\epsilon = \alpha + s_t$$

where α and s_t are the absorption and total scattering efficiencies.

3. Laboratory Measurements

A magnetic "fluidizer" was constructed by Rutstein Associates, Oberlin, Ohio, to disperse the iron fibers. This unit was extensively modified to supply solely single fibers in a gentle airflow pattern. The functional system is described in three illustrations (figures 2, 3, and 4) and their captions. The last of these figures shows the sampling systems that tap into the airflow of the fluidizer duct (10 cm diameter tube). Note that the photoacoustical and an aerosol characterization system are in series; that is, the same sample is optically measured and then collected for analysis.

The photoacoustical system was first described in Applied Optics in 1984 (Bruce and Richardson 1984) and more recently in 1991, in the same journal (Bruce et al. 1991). Photoacoustics, which measures only the absorption, is appropriate in the case of these short ($L << \lambda$), small-diameter high-conductivity fibers. Scattering will account for well under 1 percent of the extinction.

The 94 GHz absorption efficiency, measured photoacoustically in the laboratory, for separated fibers, using gentle processing in the magnetic fluidizer was

$$\alpha = 2.2 \times 10^{-1}\ m^2/g\ (1987),$$

for a length distribution peaked near 70 μm.

Another value was obtained by using a somewhat stronger fluidizer oscillating magnetic field. In this case, multiple particles were more often obtained. These particles would often partly overlap, effectively creating longer particles. Theoretically, the efficiency increases in a power-law relationship with length, $L^{3.49}$, in the "Rayleigh" region

(includes all the fibers measured) while the power-law relation for the diameter is weaker $\sim d^{-2.53}$, in the opposite direction with respect to the efficiency. Thus, a measured increase to $\alpha = 4.1 \times 10^{-1}$ m^2/g for the somewhat siamesed particles is not a surprise.

Precise comparison with the strong power law functions for the diameter and length of the theory is difficult for fibers with $kL << 1$, particularly for the diameters (k is the propagation vector). As the photographs of figure 1 show, the effective particle diameter is often not well defined, being complicated by the general "lumpiness." These fibers, like all condensate solid aerosols we have seen, started growth as spheres and coalesced when their radii were of the order of tens of nanometers. Growth then continued in this case to a mean diameter of the order of ~ 0.2 μm.

The calculational estimate was based on measured length (detailed) and diameter (approximate) distributions. Graphs of the distribution of lengths and the consequent calculated optical efficiencies are shown in figures 5 and 6.

Functional dependencies were taken from calculations based on Pedersen et al. (1985, 1987) and Waterman and Pedersen (1992). The result for the separated fibers was

$$\alpha = 1.12 \times 10^{-1} \ m^2/g.$$

Here we remind the reader that the fibers measured were separated about as gently as is possible. The system airflows were carefully managed for this (relatively low velocity and turbulence). As figure 4 shows, all measurements were made in series (photoacoustic first, then dosage and sizing from the same sample). It is not likely that longer single fibers could be extracted from the nested sample provided. Therefore, the values are probably near maximum for that material.

When the variation in diameter along the fibers is considered, the agreement between measurement and theory is quite good. Samples with longer separable fibers would provide another point validation.

4. Comments

Given the strong power-law relationships for optical efficiency functions of the two basic fiber dimensions, an increase in separable fiber length for the redispersed material would be valuable for testing the theory and should be sought. However, an altered process of generation leading to a decrease in fiber diameter of more than about a factor of 2 is unlikely. Fiber strength becomes a consideration for longer lengths and smaller diameters. At some point the joints would become too weak to allow collection and redispersion. (Soot "fibers" often have diameters of less than 0.1 μm but are very fragile.)

Even a factor of 2 decrease in diameter would increase the efficiency by about a factor of 6, according to the theory: not enough . . . by itself. Fiber length, then, is the primary candidate parameter for improvement. Theory savs that simply increasing the length by, for example, a factor of 3 yields an efficiency increase of about 50! If this length is difficult to attain, then consider an increase of only a factor of 2, which gives an efficiency improvement of 11.

The dimensional and thus optical efficiency limits for the redispersed material are therefore indirectly related to the strength of the material and the magnetic forces between adjacent fibers as they nest. This could be calculated without great complication. A small contract to quantify the dimensions for maximum optical efficiency with the bounds of material strength for ferromagnetic forces would be the quickest way to determine the potential of these fibers.

5. Field Measurements

There is an additional item of data that relates to the efficiency of this material. Measurements during a 1984 field experiment at both 140 GHz (λ = 2.14 mm) and λ = 0.63 μm gave the absorption/extinction efficiencies listed below. If the diameters are assumed to be the same as those measured in the laboratory for the study of this report, the Pedersens/Waterman theory would have it that the once-dispersed fibers of the field test were effectively only about 40 percent longer than those of our laboratory measurements (recall that they are multiply connected). The implication is that, assuming similar particles for the two situations, the fluidizer caused comparatively little breakage. In any case, the generators were not producing particles that were long enough to realize a significant portion of the iron fiber potential.

Extinction/absorption efficiencies (m^2/g) measured during field experiments of 1984.

	140 GHz	0.63 μm
Run 1	0.67	3.2
Run 2	0.79	4.2

Finally it should be noted from the above data that this would be a truly broadband absorber if the length could be increased as discussed above. This is not true for the fibers of the other category (chopped extruded fibers, Bruce et al. 1990) as their diameters preclude satisfactory efficiency in the IR.

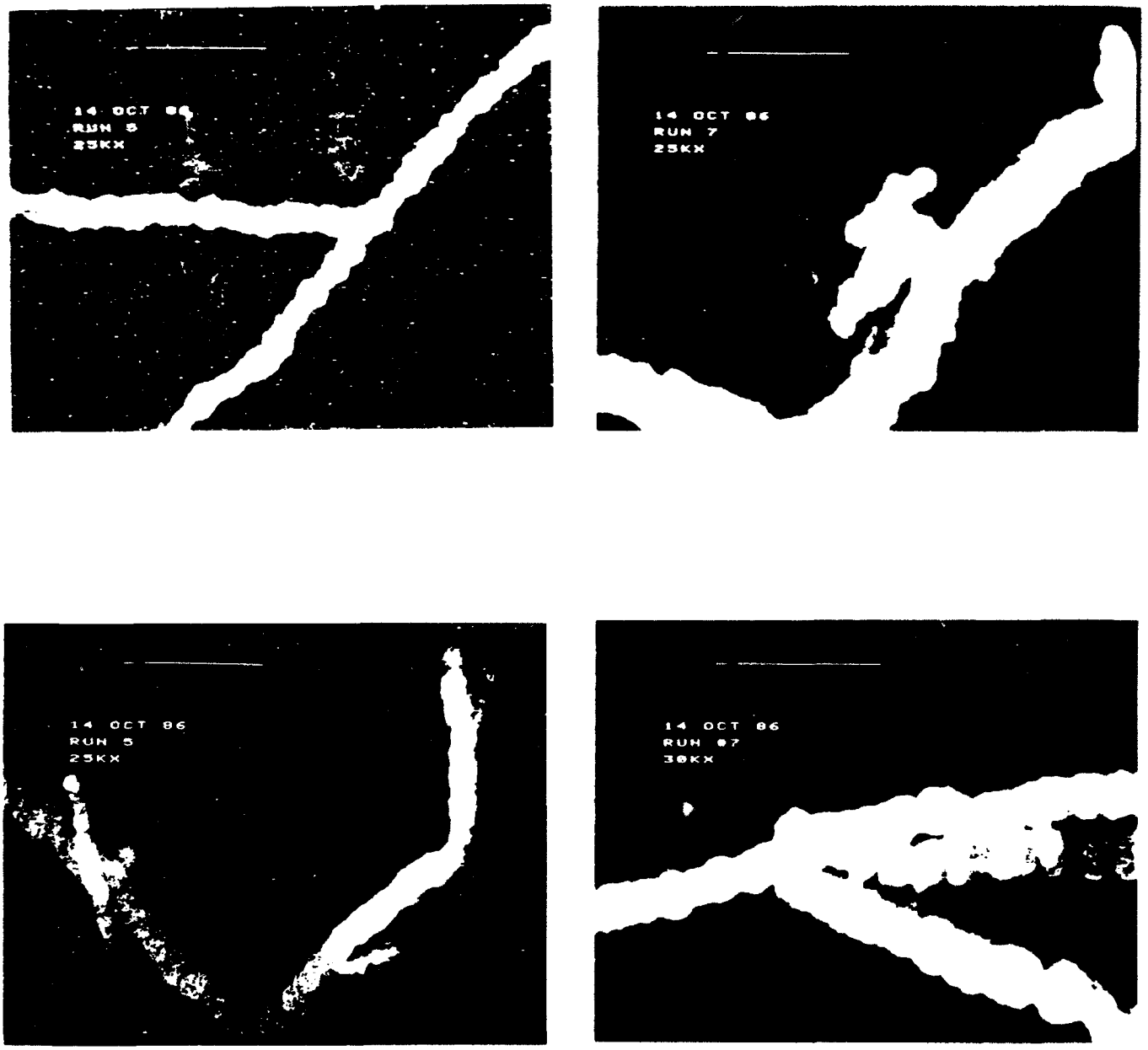

Figure 1. Scanning electron micrographs of the iron condensation particles.

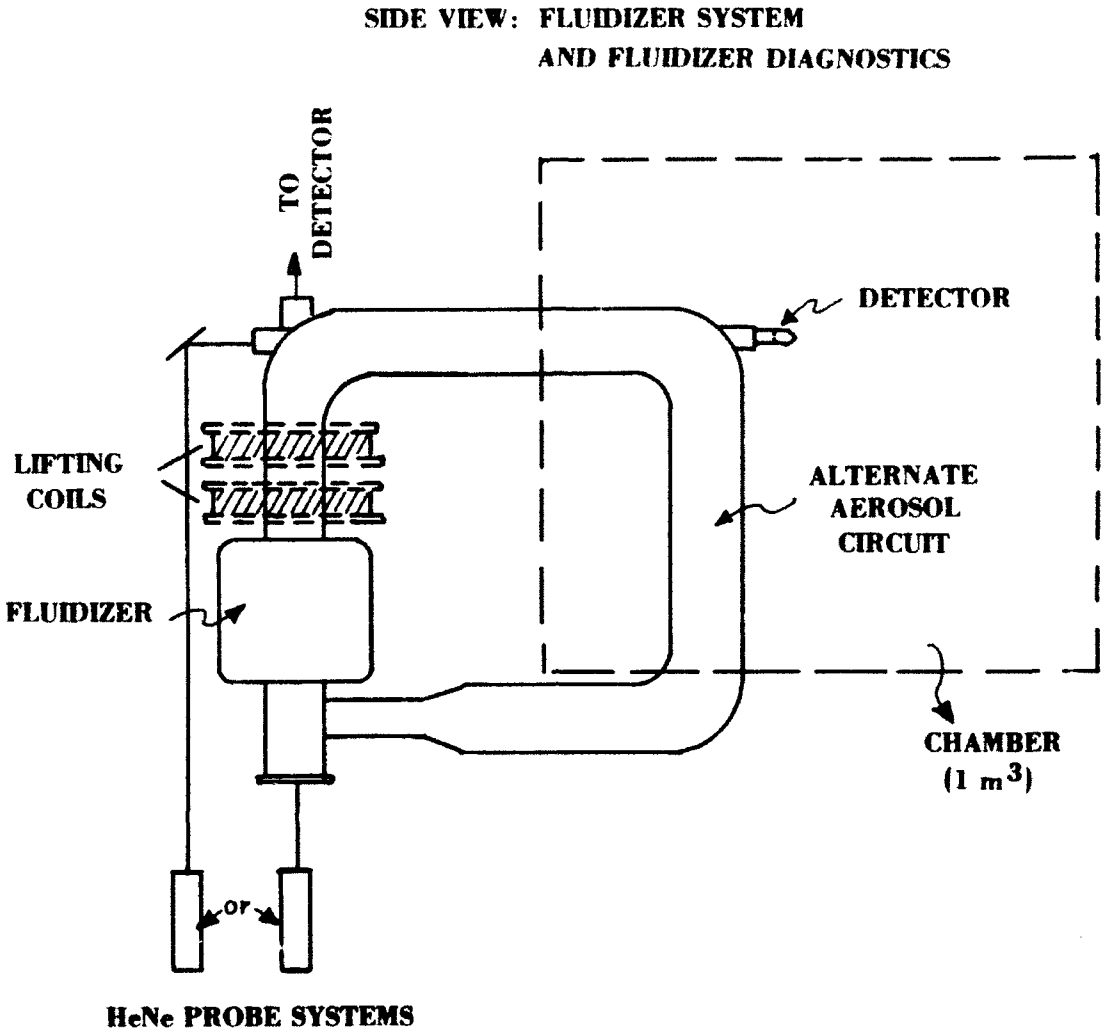

Figure 2. **Fluidizer and airflow circuit. During the laboratory study, the smaller volume (alternate) flow circuit was used. A nonintrusive flow mechanism (Alprin ejector) was installed in series in the 10-cm-diameter tubing. A sketch of the removable section at the base of the fluidizer is shown in figure 3.**

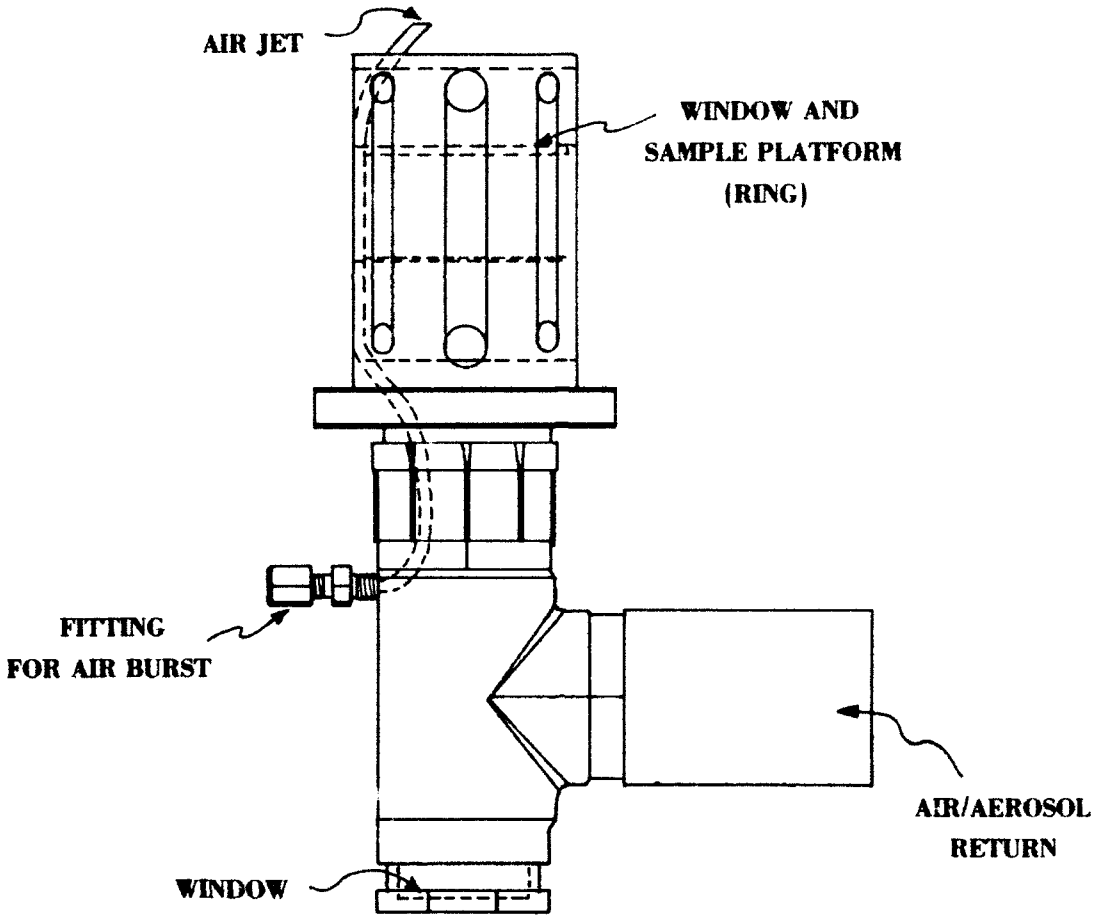

Figure 3. Removable section at base of fluidizer. This unit has several important functions. The air/aerosol returns to a plenum just underneath the glass sample holder and passes along channels that enter the fluidizer chamber above the sample platform. A glass window at the base of the plenum allows the laser probe beam to pass through the center of the fluidizer chamber after the particles have been levitated. There is also an air jet near the center of the chamber that can be used to provide bursts of air when the material is too nested to be separated by the fluidizer.

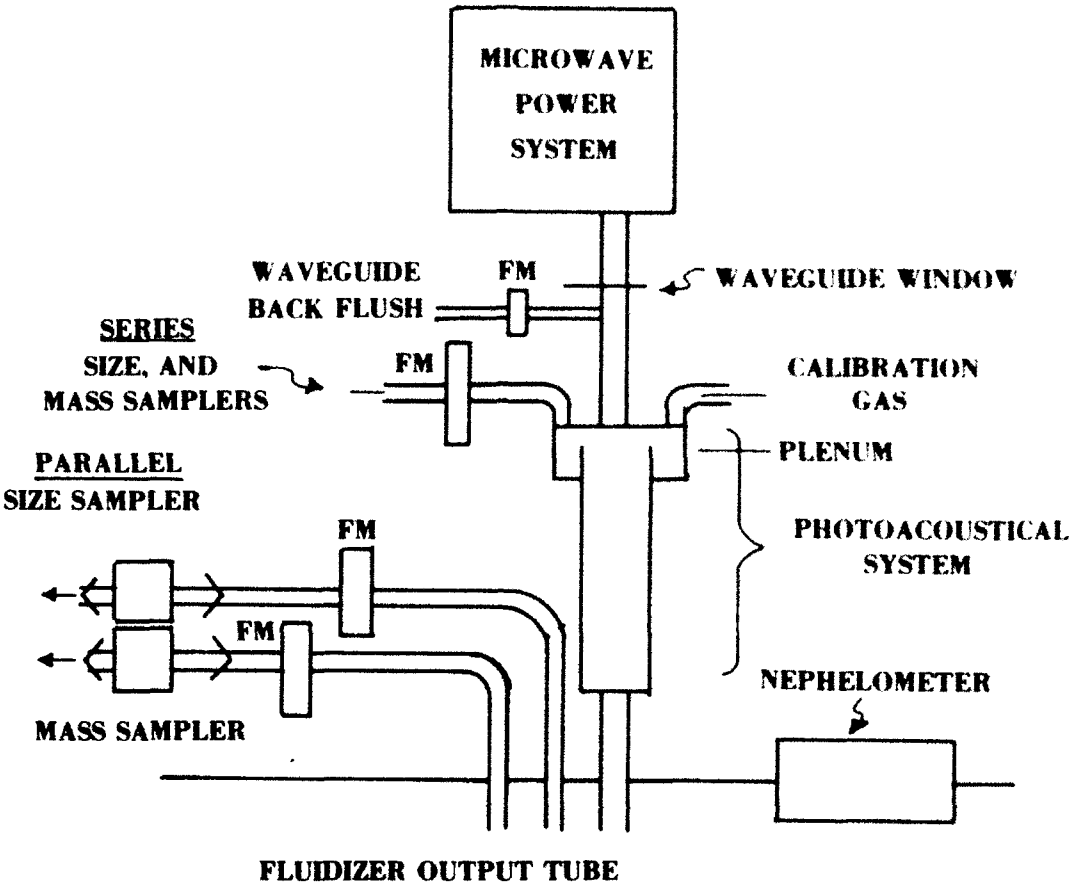

Figure 4. Microwave and aerosol characterization system. The type of microwave photoacoustical system (spectrophone) used was described some time ago by Bruce and Richardson (1984). Aerosol characterization systems were arranged in both parallel and series sampling circuits with respect to the spectrophone. The assurance of characterizing the identical sample measured photoacoustically was too strong an approach to ignore. A nephelometer operating in the near IR, sampling with the primary flow circuit, served as a reference aerosol density detector for fluidizer performance. Another nephelometer (shown) was installed in series with the spectrophone for correlation of the time dependence. Dosimetric samples were obtained on polycarbonate filters and were analyzed using atomic absorption spectroscopy (AAS). Size analyses were obtained using the same filters before the destructive AAS process. All flowmeters were calibrated using menisci of soapy water moving in a glass tube.

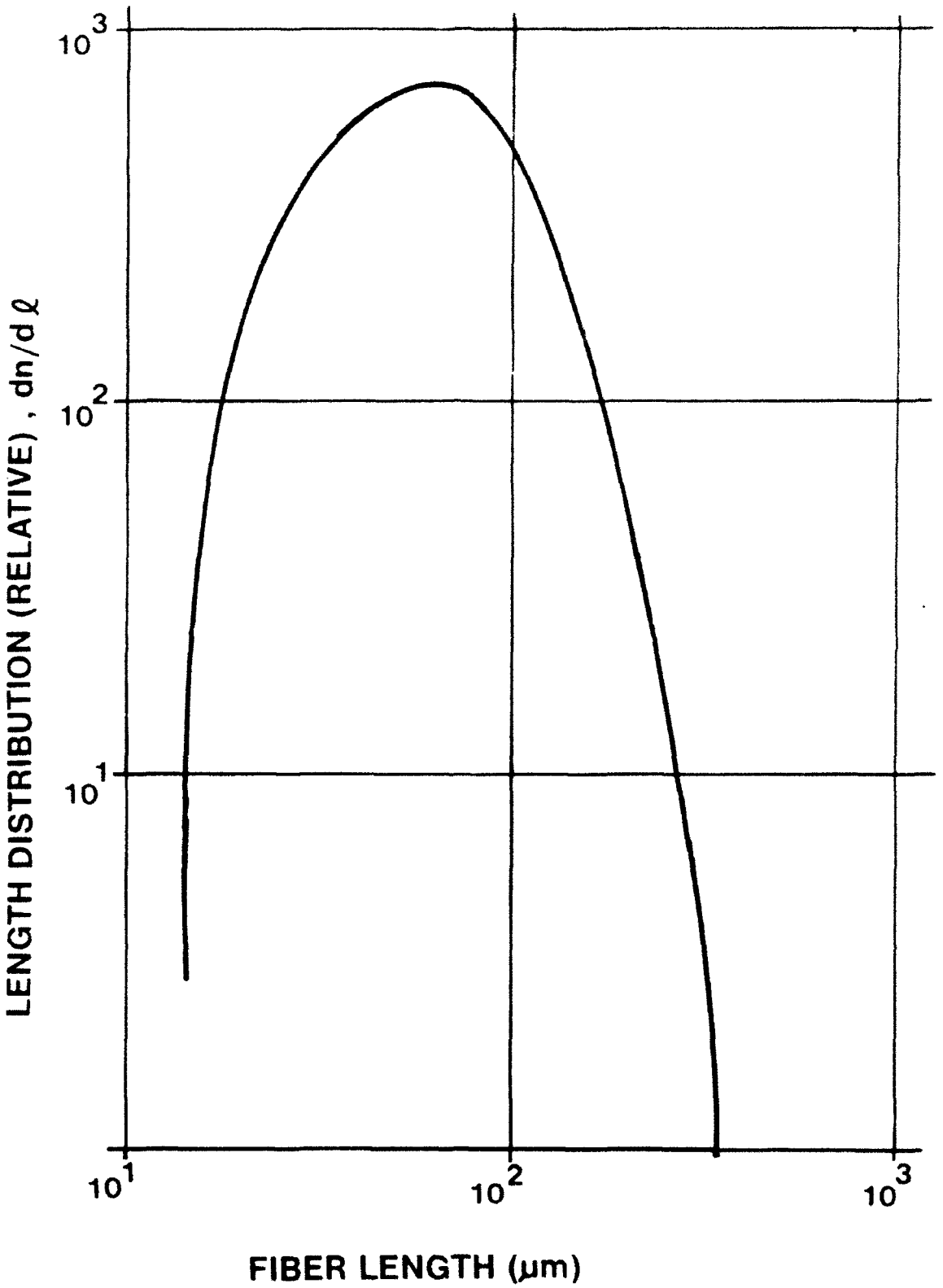

Figure 5 . Single fiber length distribution.

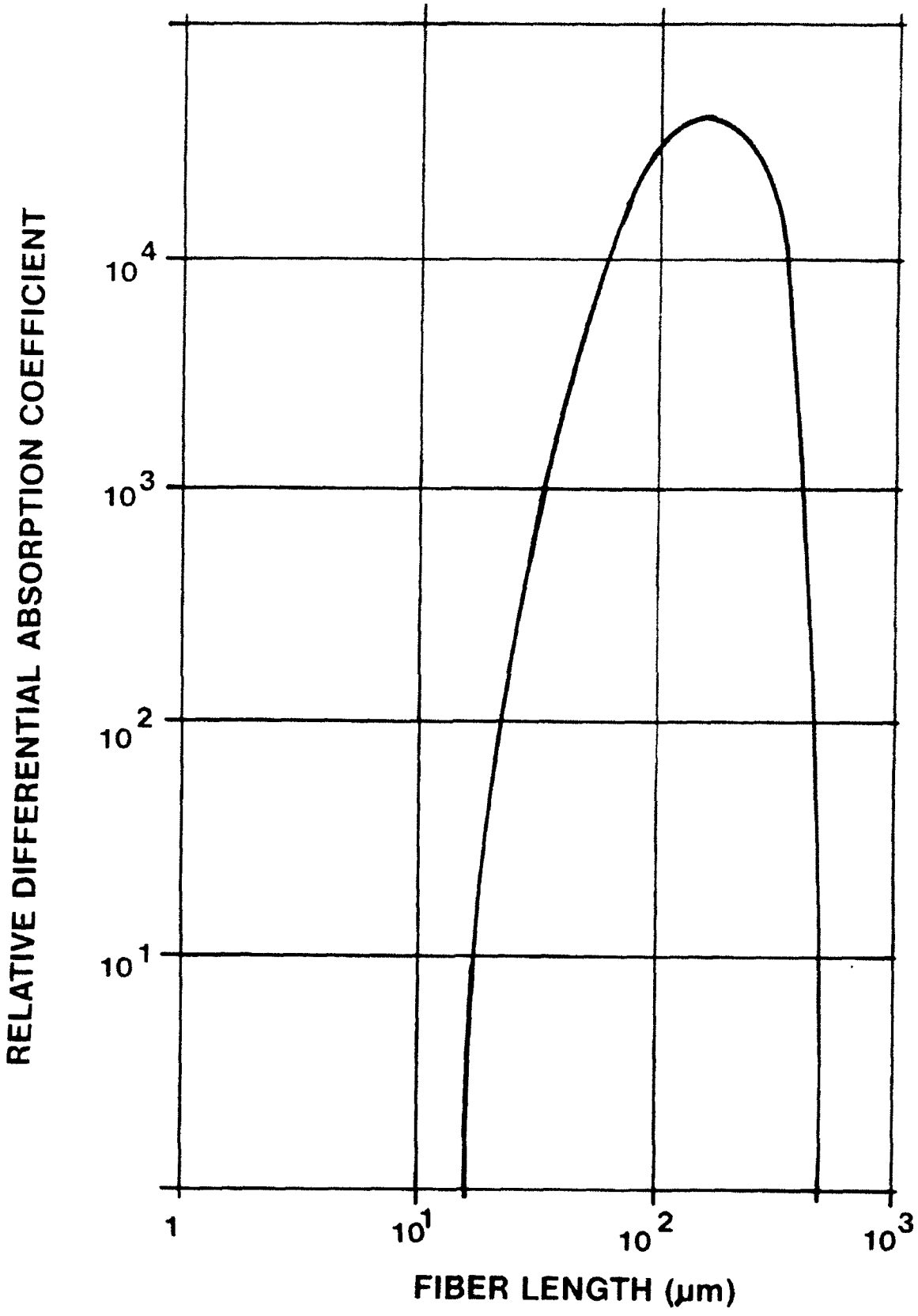

Figure 6. Calculated extinction, absorption with length.

Literature Cited

Bruce, C. W., T. F. Stromberg, K. P. Gurton, and J. B. Mozer, 1991, Trans-Spectral Absorption and Scattering of Electromagnetic Radiation of Diesel Soot, Appl Opt, 30:1537.

Bruce, C. W., D. R. Ashmore, P. C. Pittman, N. E. Pedersen, J. C. Pedersen, and P. C. Waterman, 1990a, Attenuation at a Wavelength of 0.86 cm Due to Fibrous Aerosols, Appl Phys Letters, 56:791.

Bruce, C. W., A. V. Jelinek, R. M. Halonen, and M. J. Stehling, 1990b, Millimeter Wavelength Attenuation Efficiencies of Fibrous Aerosols, Proceedings of the Smoke/Obscurants Symposium XIV, CRDEC, ATTN: SMCCR-MUM, Aberdeen Proving Ground, Maryland 21010-5423, 119-126.

Bruce, C. W., and N. M. Richardson, 1984, Millimeter Wavelength Gas/Aerosol Spectrophone and Application to Diesel Smoke, Appl Opt, 23:13.

Pedersen, N. E., J. C. Pedersen, and P. C. Waterman, 1985, Absorption and Scattering by Conductive Fibers: Basic Theory and Comparison with Asymptotic Results, USAF Contract Report F49620-84-C-0045, Air Force Office of Scientific Research, building 410, Bolling Air Force Base, Washington, DC 20332-6448.

Pedersen, N. E., P. C. Waterman, and J. C. Pedersen, 1987, Absorption Scattering and Thermal Radiation by Conductive Fibers, USAF Contract Report F49620-84-C-0045, Air Force Office of Scientific Research, building 410, Bolling Air Force Base, Washington, DC 20332-6448.

van de Hulst, H. C., 1957, Light Scattering by Small Particles, Wiley, New York.

Waterman, P. C., and J. C. Pedersen, 1992, Scattering by Finite Wires, Appl Phys, 72:349-357.

DISTRIBUTION LIST FOR PUBLIC RELEASE

Commandant
U.S. Army Chemical School
ATTN: ATZN-CM-CC (S. Barnes)
Fort McClellan, AL 36205-5020

NASA/Marshall Space Flight Center
Deputy Director
Space Science Laboratory
Atmospheric Sciences Division
ATTN: ES01 (Dr. George H. Fichtl)
Huntsville, AL 35812

NASA/Marshall Space Center
ATTN: Code ES44 (Dale Johnson)
Huntsville, AL 35812

NASA/Marshall Space Flight Center
Atmospheric Sciences Division
ATTN: Code ED-41
Huntsville, AL 35812

Deputy Commander
U.S. Army Strategic Defense Command
ATTN: CSSD-SL-L
Dr. Julius Q. Lilly
P.O. Box 1500
Huntsville, AL 35807-3801

Commander
U.S. Army Missile Command
ATTN: AMSMI-RD-AC-AD
Donald R. Peterson
Redstone Arsenal, AL 35898-5242

Commander
U.S. Army Missile Command
ATTN: AMSMI-RD-AS-SS
Huey F. Anderson
Redstone Arsenal, AL 35898-5253

Commander
U.S. Army Missile Command
ATTN: AMSMI-RD-AS-SS
B. Williams
Redstone Arsenal, AL 35898-5253

Commander
U.S. Army Missile Command
ATTN: AMSMI-RD-DE-SE
Gordon Lill, Jr.
Redstone Arsenal, AL 35898-5245

Commander
U.S. Army Missile Command
Redstone Scientific Information Center
ATTN: AMSMI-RD-CS-R/Documents
Redstone, Arsenal, AL 35898-5241

Commander
U.S. Army Intelligence Center and Fort Huachuca
ATTN: ATSI-CDC-C (Mr. Colanto)
Fort Huachuca, AZ 85613-7000

Northrup Corporation
Electronics Systems Division
ATTN: Dr. Richard D. Tooley
2301 West 120th Street, Box 5032
Hawthorne, CA 90251-5032

Commander - Code 3331
Naval Weapons Center
ATTN: Dr. Alexis Shlanta
China Lake, CA 93555

Commander
Pacific Missile Test Center
Geophysics Division
ATTN: Code 3250 (Terry E. Battalino)
Point Mugu, CA 93042-5000

Lockheed Missiles & Space Co., Inc.
Kenneth R. Hardy
Org/91-01 B/255
3251 Hanover Street
Palo Alto, CA 94304-1191

Commander
Naval Ocean Systems Center
ATTN: Code 54 (Dr. Juergen Richter)
San Diego, CA 92152-5000

Meteorologist in Charge
Kwajalein Missile Range
P.O. Box 67
APO San Francisco, CA 96555

U.S. Department of Commerce
Mountain Administration Support
Center
Library, R-51 Technical Reports
325 S. Broadway
Boulder, CO 80303

Dr. Hans J. Liebe
NTIA/ITS S 3
325 S. Broadway
Boulder, CO 80303

NCAR Library Serials
National Center for Atmos Rsch
P.O. Box 3000
Boulder, CO 80307-3000

HQDA
ATTN: DAMI-POI
Washington, DC 20310-1067

Mil Asst for Env Sci Ofc of
The Undersecretary of Defense
for Rsch & Engr/R&AT/E&LS
Pentagon - Room 3D129
Washington, DC 20301-3080

HQDA
DEAN-RMD/Dr. Gomez
Washington, DC 20314

Director
Division of Atmospheric Science
National Science Foundation
ATTN: Dr. Eugene W. Bierly
1800 G. Street, N.W.
Washington, DC 20550

Commander
Space & Naval Warfare System Command
ATTN: PMW-145-1G (LT Painter)
Washington, DC 20362-5100

Commandant
U.S. Army Infantry
ATTN: ATSH-CD-CS-OR
Dr. E. Dutoit
Fort Benning, GA 30905-5090

USAFETAC/DNE
Scott AFB, IL 62225

Air Weather Service
Technical Library - FL4414
Scott AFB, IL 62225-5458

USAFETAC/DNE
ATTN: Mr. Charles Glauber
Scott AFB, IL 62225-5008

Commander
U.S. Army Combined Arms Combat
ATTN: ATZL-CAW (LTC A. Kyle)
Fort Leavenworth, KS 66027-5300

Commander
U.S. Army Space Institute
ATTN: ATZI-SI (Maj Koepsell)
Fort Leavenworth, KS 66027-5300

Commander
U.S. Army Space Institute
ATTN: ATZL-SI-D
Fort Leavenworth, KS 66027-7300

Commander
Phillips Lab
ATTN: PL/LYP (Mr. Chisholm)
Hanscom AFB, MA 01731-5000

Director
Atmospheric Sciences Division
Geophysics Directorate
Phillips Lab
ATTN: Dr. Robert A. McClatchey
Hanscom AFB, MA 01731-5000

Raytheon Company
Dr. Charles M. Sonnenschein
Equipment Division
528 Boston Post Road
Sudbury, MA 01776
Mail Stop 1K9

Director
U.S. Army Materiel Systems
Analysis Activity
ATTN: AMXSY-MP (H. Cohen)
APG, MD 21005-5071

Commander
U.S. Army Chemical Rsch,
Dev & Engr Center
ATTN: SMCCR-OPA (Ronald Pennsyle)
APG, MD 21010-5423

Commander
U.S. Army Chemical Rsch,
Dev & Engr Center
ATTN: SMCCR-RS (Mr. Joseph Vervier)
APG, MD 21010-5423

Commander
U.S. Army Chemical Rsch,
Dev & Engr Center
ATTN: SMCCR-MUC (Mr. A. Van De Wal)
APG, MD 21010-5423

Director
U.S. Army Materiel Systems
Analysis Activity
ATTN: AMXSY-AT (Mr. Fred Campbell)
APG, MD 21005-5071

Director
U.S. Army Materiel Systems
Analysis Activity
ATTN: AMXSY-CR (Robert N. Marchetti)
APG, MD 21005-5071

Director
U.S. Army Materiel Systems
Analysis Activity
ATTN: AMXSY-CS (Mr. Brad W. Bradley)
APG, MD 21005-5071

Director
U.S. Army Research Laboratory
ATTN: AMSRL-D
2800 Powder Mill Road
Adelphi, MD 20783

Director
U.S. Army Research Laboratory
ATTN: AMSRL-OP-CI-A
(Technical Publishing)
2800 Powder Mill Road
Adelphi, MD 20783

Director
U.S. Army Research Laboratory
ATTN: AMSRL-OP-CI-AD, Record Copy
2800 Powder Mill Road
Adelphi, MD 20783

Director
U.S. Army Research Laboratory
ATTN: AMSRL-SS-SH
Dr. Z.G. Sztankay
2800 Powder Mill Road
Adelphi, MD 20783

National Security Agency
ATTN: W21 (Dr. Longbothum)
9800 Savage Road
Ft George G. Meade, MD 20755-6000

U. S. Army Space Technology
and Research Office
ATTN: Brenda Brathwaite
5321 Riggs Road
Gaithersburg, MD 20882

OIC-NAVSWC
Technical Library (Code E-232)
Silver Springs, MD 20903-5000

The Environmental Research
Institute of Michigan
ATTN: IRIA Library
P.O. Box 134001
Ann Arbor, MI 48113-4001

Commander
U.S. Army Research Office
ATTN: DRXRO-GS (Dr. W.A. Flood)
P.O. Box 12211
Research Triangle Park, NC 27709

Dr. Jerry Davis
North Carolina State University
Department of Marine, Earth, &
Atmospheric Sciences
P.O. Box 8208
Raleigh, NC 27650-8208

Commander
U. S. Army CECRL
ATTN: CECRL-RG (Dr. H. S. Boyne)
Hanover, NH 03755-1290

Commanding Officer
U.S. Army ARDEC
ATTN: SMCAR-IMI-I, Bldg 59
Dover, NJ 07806-5000

U.S. Army Communications-Electronics
Command EW/RSTA Directorate
ATTN: AMSEL-RD-EW-OP
Fort Monmouth, NJ 07703-5206

Commander
U.S. Army Satellite Comm Agency
ATTN: DRCPM-SC-3
Fort Monmouth, NJ 07703-5303

6585th TG (AFSC)
ATTN: RX (CPT Stein)
Holloman AFB, NM 88330

Department of the Air Force
OL/A 2nd Weather Squadron (MAC)
Holloman AFB, NM 88330-5000

PL/WE
Kirtland AFB, NM 87118-6008

Director
U.S. Army TRADOC Analysis Command
ATTN: ATRC-WSS-R
White Sands Missile Range, NM 88002

USAF Rome Laboratory Technical
Library, FL2810 Corridor W, Site 262,
RL//SUL (DOCUMENTS LIBRARY)
26 Electronics Parkway, Bldg 106
Griffiss AFB, NY 13441-4514

AFMC/DOW
Wright-Patterson AFB, OH 0334-5000

Commandant
U.S. Army Field Artillery School
ATTN: ATSF-TSM-TA
Mr. Charles Taylor
Fort Sill, OK 73503-5600

Commander
Naval Air Development Center
ATTN: Al Salik (Code 5012)
Warminister, PA 18974

Commander
U.S. Army Dugway Proving Ground
ATTN: STEDP-MT-DA-M
Mr. Paul Carlson
Dugway, UT 84022

Commander
U.S. Army Dugway Proving Ground
ATTN: STEDP-MT-DA-L
Dugway, UT 84022

Commander
U.S. Army Dugway Proving Ground
ATTN: STEDP-MT-M (Mr. Bowers)
Dugway, UT 84022-5000

Defense Technical Information Center
ATTN: DTIC-FDAC (2)
Cameron Station
Alexandria, VA 22314

Commanding Officer
U.S. Army Foreign Science &
Technology Center
ATTN: CM
220 7th Street, NE
Charlottesville, VA 22901-5396

Naval Surface Weapons Center
Code G63
Dahlgren, VA 22448-5000

Commander
U.S. Army OEC
ATTN: CSTE-EFS
Park Center IV
4501 Ford Ave
Alexandria, VA 22302-1458

Commander and Director
U.S. Army Corps of Engineers
Engineer Topographics Laboratory
ATTN: ETL-GS-LB
Fort Belvoir, VA 22060

TAC/DOWP
Langley AFB, VA 23665-5524

U.S. Army Topo Engineering Center
ATTN: CETEC-ZC
Fort Belvoir, VA 22060-5546

Commander
Logistics Center
ATTN: ATCL-CE
Fort Lee, VA 23801-6000

Commander
USATRADOC
ATTN: ATCD-FA
Fort Monroe, VA 23651-5170

Science and Technology
101 Research Drive
Hampton, VA 23666-1340

Commander
U.S. Army Nuclear & Cml Agency
ATTN: MONA-ZB Bldg 2073
Springfield, VA 22150-3198